Conserved residues modulate copper release in human copper chaperone Atox1

Faiza Hussain*, John S. Olson*†, and Pernilla Wittung-Stafshede*†‡§

*Department of Biochemistry and Cell Biology, †Keck Center for Structural Computational Biology, and ‡Department of Chemistry, Rice University, 6100 Main Street, Houston, TX 77251

Edited by Harry B. Gray, California Institute of Technology, Pasadena, CA, and approved May 2, 2008 (received for review March 25, 2008)

It is unclear how the human copper (Cu) chaperone Atox1 delivers Cu to metal-binding domains of Wilson and Menkes disease proteins in the cytoplasm. To begin to address this problem, we have characterized Cu(I) release from wild-type Atox1 and two point mutants (Met_{10}Ala and Lys_{60}Ala). The dynamics of Cu(I) displacement from holo-Atox1 were measured by using the Cu(I) chelator bicinchonic acid (BCA) as a metal acceptor. BCA removes Cu(I) from Atox1 in a three-step process involving the bimolecular formation of an initial Atox1–Cu–BCA complex followed by dissociation of Atox1 and the binding of a second BCA to generate apo-Atox1 and Cu–BCA_2. Both mutants lose Cu(I) more readily than wild-type Atox1 because of more rapid and facile displacement of the protein from the Atox1–Cu–BCA intermediate by the second BCA. Remarkably, Cu(I) uptake from solution by BCA is much slower than the transfer from holo-Atox1, presumably because of slow dissociation of DTT–Cu complexes. These results suggest that Cu chaperones play a key role in making Cu(I) rapidly accessible to substrates and that the activated protein–metal–chelator complex may kinetically mimic the ternary chaperone–metal–target complex involved in Cu(I) transfer *in vivo*.

Wilson disease protein | Menkes disease protein | stopped-flow mixing | Cu-binding mechanism | Cu transfer

Copper (Cu) is one of the most prevalent transition metals in living organisms (1). Because free copper is toxic, copper homeostasis in living organisms is tightly controlled by molecular mechanisms in which the metal is sequestered by protein carriers (2–4). During the past decade, an important class of cytoplasmic copper chaperones have been identified that bind Cu(I) with Cys_2 coordination (5–9). These small, soluble proteins guide and protect the copper ions within the cell, delivering them to the appropriate functional targets. In humans, the Cu(I) chaperone Atox1 delivers Cu to metal-binding domains of ATP7A (i.e., Menkes disease protein) and ATP7B (i.e., Wilson disease protein) proteins, which are P_{1B}-type ATPases (6, 7, 10). In an ATP-dependent process, ATP7A or ATP7B (depending on the cell type) translocate copper from the cytoplasm into the Golgi lumen for insertion into enzymes in the secretory pathway (6), such as apo-ceruloplasmin (11).

Human Atox1 is a 68-residue protein that, like the metal-binding domains in ATP7A and ATP7B, has a ferredoxin-like α/β-fold and a single M*X*C*XX*C copper-binding motif (12, 13) (Fig. 1*A*). Structural work has demonstrated that Cu chaperones and target metal-binding domains from various organisms possess the same fold and coordinate the metal via two surface-exposed cysteines in the M*X*C*XX*C motif (13–21). Although the methionine in the first position of the M*X*C*XX*C motif is conserved in all organisms, it is not directly involved in metal ligation (13). Instead, it has been proposed to act as a tether that modulates copper-binding loop structure (13, 22).

An important difference between the eukaryotic and bacterial Cu chaperones is the amino acid at position 60. Although distant in primary sequence from the metal-binding site, this residue is situated in close proximity to the metal-binding site in the tertiary structure. In eukaryotic Cu chaperones, including Atox1, this residue is an invariant Lys, which is proposed to neutralize the overall negative charge of the Cu-thiolate center (13). In prokaryotes, the amino acid at the position corresponding to 60 in Atox1 is always a Tyr that forms hydrophobic contacts with the side chain of the conserved methionine in the metal-binding motif (13). Atox1, like the other Cu chaperones, binds Cu(I) with a linear S-Cu-S coordination, although a three-coordinate adduct has also been detected in the presence of external ligands, such as DTT (23).

The affinity of Atox1 for Cu(I) is reported to be in the range of 10^6 to 10^{10} M^{-1}, and similar Cu affinities of target domains in ATP7A and ATP7B have been determined (24, 25). Thus, vectorial Cu transfer from the chaperone to the target domain does not appear to be driven by thermodynamics. Instead, Cu transport occurs by the ATP-dependent net irreversible transport of the metal into the secretory vesicles, which is facilitated by specific donor–acceptor protein interactions (18, 24).

To begin to address the mechanism of Cu(I) transfer between Atox1 and target domains, we have here examined the role of two conserved residues (Met-10 and Lys-60) in Atox1 Cu transfer reactions, by using the Cu(I) chelator bicinchonic acid (BCA), as a metal displacement reagent. The displacement of Cu from holo-Atox1 by BCA involves a three-step reaction. The initial bimolecular step forms a transient Atox1–Cu–BCA species, and then Atox1 is displaced from the metal by a second BCA molecule. The mutations of Met-10 and Lys-60 to alanines markedly enhance the rate and extent of Cu transfer from Atox1 to BCA. Thus, the native Met and Lys residues do play a key role in Cu retention in Atox1, even though they are not ligands of the metal.

Results

Characterization of Atox1 Variants Met_{10}Ala and Lys_{60}Ala. The Met_{10}Ala and Lys_{60}Ala Atox1 mutants were constructed, expressed, and purified as described in *Materials and Methods*. The positions of these amino acids in the solution structure of Atox1 are shown in Fig. 1*A*. The apo forms of both Atox1 variants are folded based on their far-UV circular dichroism (CD) signals (Fig. 1*B*). Fluorescence spectra also confirm folded structures for the variants (data not shown; mutant spectra exhibit the same Tyr emission at 303 nm as wild-type Atox1). Based on analysis of the CD spectra by the program Dichroweb (26), all three proteins have 66–68% helical and 14–18% β-sheet content plus 16–20% loop and unordered regions. Cu interaction with Atox1 can be monitored via near-UV CD (27). For both Atox1 variants, Cu binds to the proteins as indicated by similar near-UV CD

Author contributions: F.H. and P.W.-S. designed research; F.H. performed research; F.H., J.S.O., and P.W.-S. analyzed data; and J.S.O. and P.W.-S. wrote the paper.

The authors declare no conflict of interest.

This article is a PNAS Direct Submission.

§To whom correspondence should be sent at the present address: Department of Chemistry, Umeå University, SE-901 87 Umeå, Sweden. E-mail: pernilla.wittung@chem.umu.se.

This article contains supporting information online at www.pnas.org/cgi/content/full/0802928105/DCSupplemental.

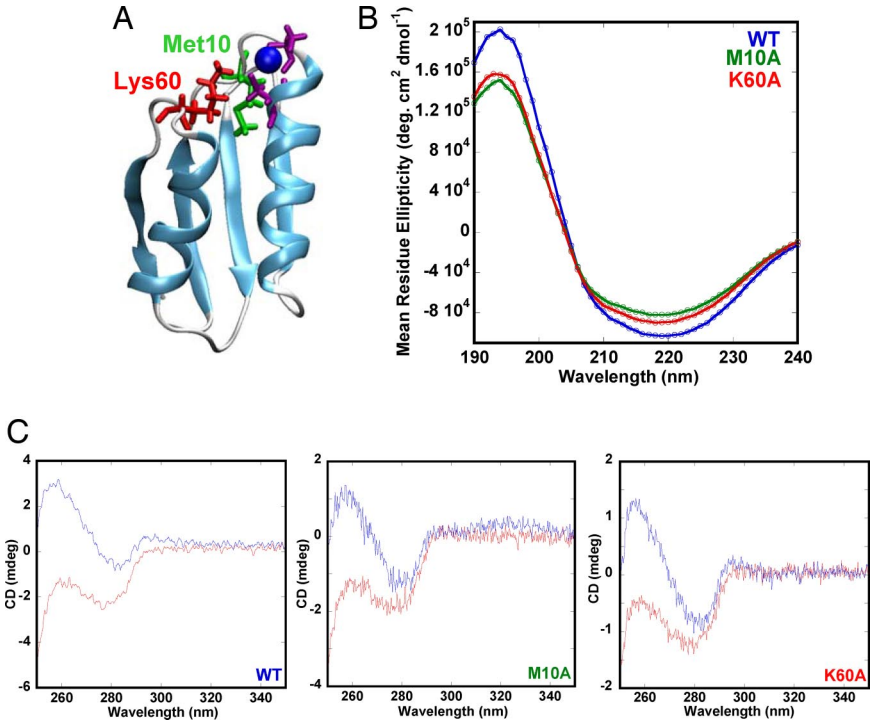

Fig. 1. Structure and Cu-binding of Atox1 variants. (*A*) Structure (Protein Data Bank code 1TL4) of human Atox1. Cu is blue, the two metal-binding Cys are purple, and Met-10 and Lys-60 are green and red, respectively. Both Met-10 and Lys-60 are within 4 Å of the Cu. (*B*) Far-UV CD of wild-type (blue), $Met_{10}Ala$ (green), and $Lys_{60}Ala$ (red) Atox1 (30 μM protein, 5 mM phosphate, pH 7.5, 20°C). (*C*) Near-UV CD of Atox1 variants (*Left*, wild-type; *Center*, $Met_{10}Ala$; *Right*, $Lys_{60}Ala$) in the apo (red) and holo (blue) forms (20 mM Tris, 150 mM NaCl, 0.25 mM DTT, pH 7.5, 20°C).

changes upon additions of one equivalent of Cu (Fig. 1*C*). Titration of Cu to all three proteins resulted in saturation of the changes at 1:1 ratio (data not shown).

Atox1–Cu Dissociation Kinetics. To measure the rate of Cu dissociation from Atox1, the holoprotein was mixed with increasing amounts of the Cu chelator BCA. BCA is a high affinity Cu(I) chelator that forms a colored Cu–BCA_2 species ($\log K_{stability}$ is reported to be ≈14) (28, 29). Time courses for Cu transfer were monitored by the increase in absorption at 565 nm resulting from the formation of the *bis*–BCA–Cu complex, with the use of wild-type Cu–Atox1 or "free" Cu as donors (Fig. 2 *A* and *B*).

Unexpectedly, Cu transfer from Atox1 to excess BCA was significantly faster than the uptake of "free" Cu from solution, but the extent of uptake of "free" copper from solution was much greater at all of the BCA concentrations used (Fig. 2*C*). In contrast, a 5,000-fold excess of BCA was required for complete extraction of Cu from 3 μM holo-Atox1. All of the Cu transfer experiments were performed in the presence of 0.5 mM DTT to keep Cu in the +1 state; it is probable that slow

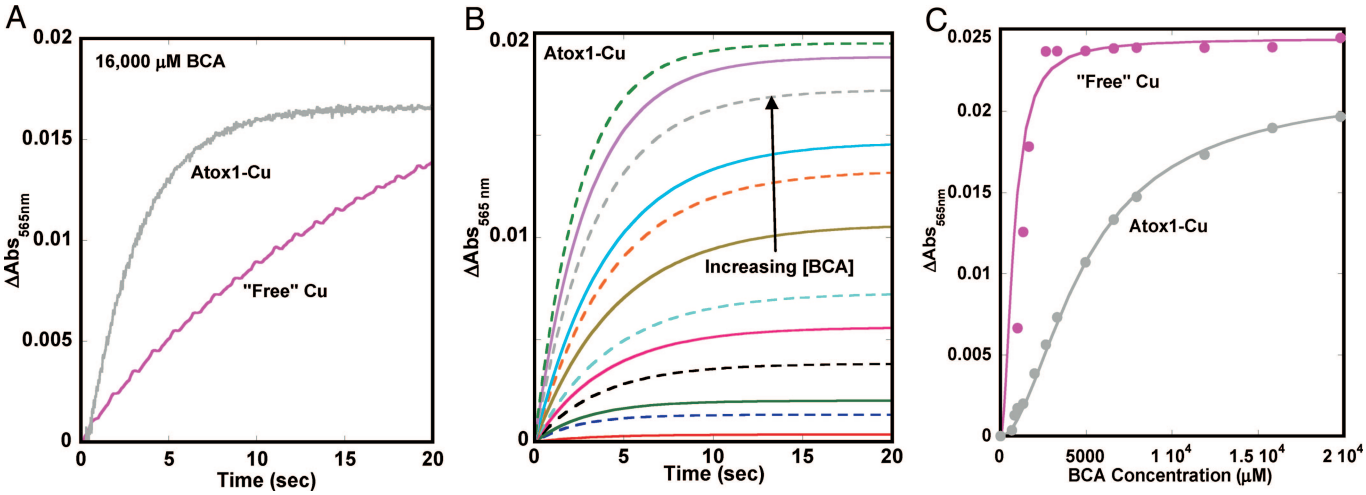

Fig. 2. Cu transfer from Atox1 and solution to BCA. (*A*) Obseved data for Cu transfer to BCA from 3 μM Atox1 and 3 μM "free" Cu at 16,000 μM BCA. (*B*) Fitted curves for transfer of Cu from wild-type Cu–Atox1 to BCA measured by absorption changes at 565 nm as a function of time (20 mM Tris, 150 mM NaCl, 0.5 mM DTT, pH 7.5, 20°C). (*C*) Amplitude change as a function of BCA concentration for Cu transfer from Atox1 and from solution.

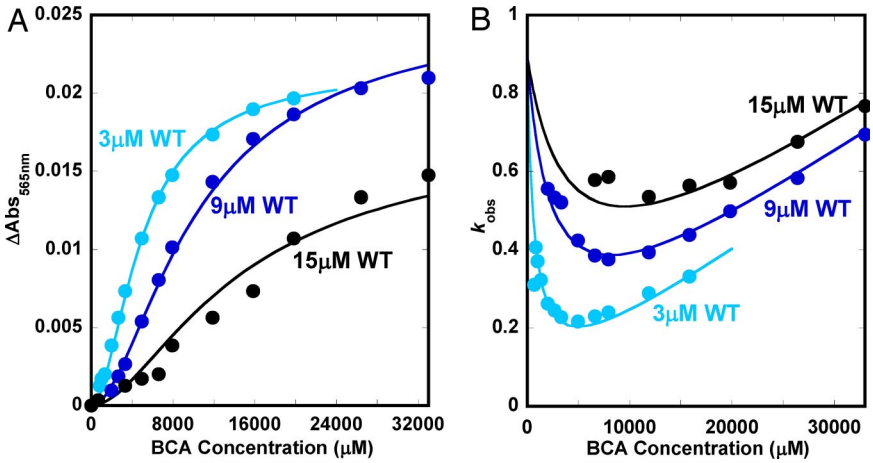

Fig. 3. Experimental (filled circles) and theoretical (solid lines) data for Cu transfer from wild-type Atox1 at approximately 1:1 (cyan blue), 1:3 (dark blue), and 1:5 (black) Cu-to-protein ratios (i.e., 3, 9, and 15 μM protein) as a function of BCA concentration. Amplitude changes (*A*) and k_{obs} (*B*) as functions of BCA concentration are shown. The theoretical curves are based on a simultaneous global fit to all of the data based on the three-step mechanism (see the text).

dissociation of DTT from Cu impedes the rate of uptake by BCA (Fig. 2*A*).

To examine the mechanism of Cu transfer from Atox1 to BCA, we measured time courses for the reaction of Atox1–Cu with BCA and varied the concentration of apo-Atox1. As shown in Fig. 3*A*, the absorbance changes occurring during titration of holo-Atox1 with BCA show a complex sigmoidal dependence on the concentration of added chelating agent. The concentration of BCA required for half-removal of copper is quite large ($\geq$5,000 μM) and increases markedly when excess apo-Atox1 is added to compete with the chelating agent for the metal. The kinetic results are even more striking. The observed rate of Cu transfer, k_{obs}, has a parabolic dependence on [BCA] (Fig. 3*B*), and this quadratic dependence is more pronounced at lower apo-Atox1 concentrations. After an initial decrease with increasing [BCA], the observed rate begins to show a linear dependence on BCA concentration. This dependence implies that, at high levels of the chelator, the process becomes second order and is not directly limited by the first order dissociation of Cu from Atox1.

Cu Dissociation from Mutant Atox1. We also performed kinetic experiments for Cu transfer from the Met_{10}Ala and Lys_{60}Ala Atox1 mutants and found the same general equilibrium and kinetic patterns (Fig. 4). For both mutants, but not wild-type Atox1, a minor slow phase was detected in the time courses for Cu–BCA_2 formation. This phase was not included in the analysis and appears to be attributable to the presence of some "free" Cu in the mutant holoprotein solutions. The rates of this slow process matched that for BCA uptake of "free" Cu in solution, shown in Fig. 2*B*. In support of this interpretation, separate dialysis experiments (data not shown) revealed that the mutants have lower affinities for Cu under these solution conditions than wild-type Atox1. The data in Fig. 4 demonstrate that both the speed and extent of Cu transfer at a given [BCA] are much greater for the mutants than for wild-type holo-Atox1. In addition, both the sigmoidal nature of the equilibrium curve and the parabolic dependence of k_{obs} on [BCA] are more pronounced for the mutants, and the apparent bimolecular rate constants for Cu transfer from the mutants at high [BCA] are much greater than that for wild-type Atox1 (slope of k_{obs} vs. [BCA], Fig. 4*B*).

Mechanistic Analysis of Cu Kinetics. The sigmoidal dependence of the equilibrium fraction of transfer on [BCA] and the parabolic dependence of the observed rate constant on [BCA] for the reaction of Atox1–Cu with excess BCA requires a mechanism with at least two distinct steps: (*i*) the transient formation of an initial ternary complex of Atox1–Cu–BCA; and (*ii*) reaction with

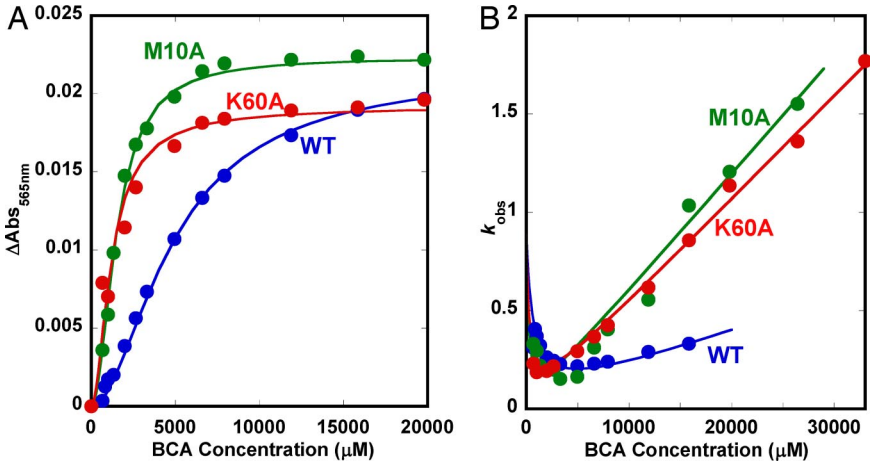

Fig. 4. Experimental (closed circles) and theoretical (solid lines) data for Cu transfer from wild-type (blue), Met_{10}Ala (green), and Lys_{60}Ala (red) Atox1 to BCA. Amplitude changes (*A*) and k_{obs} (*B*) as functions of BCA concentration are shown. The fits are based on the three-step mechanism (parameters reported in Table 1).

Table 1. Cu release from Atox1 via BCA chelation

Atox1	K_1, μM^{-1}	k_1, $\mu M^{-1}s^{-1}$	k_{-1}, s^{-1}	K_2, μM	k_2, s^{-1}	k_{-2}, $\mu M^{-1}s^{-1}$	K_3, μM^{-1}	k_3, $\mu M^{-1}s^{-1}$	k_{-3}, s^{-1}
Wild-type	7.1×10^{-5}	9.8×10^{-5}	1.4	8.5×10^{-4}	0.31	3.7×10^{2}	1.7	1.5	0.89
$Met_{10}Ala$	4.3×10^{-5}	14×10^{-5}	3.2	1.2×10^{-2}	2.4	2.0×10^{2}	1.7	1.5	0.89
$Lys_{60}Ala$	27×10^{-5}	7.3×10^{-5}	0.27	3.7×10^{-3}	0.72	2.0×10^{2}	1.7	1.5	0.89

Summary of equilibrium and kinetic parameters obtained from global fitting of amplitude and rate data for each Atox1 variant (Fig. 4) by using the equations given in the text that are based on the three-step mechanism.

a second BCA molecule to displace apoAtox1 and generate the strongly absorbing *bis*–BCA–Cu complex [see supporting information (SI) Fig. S1].

Simple dissociation of Cu from holo-Atox1 and then reaction of "free" Cu in solution with BCA cannot explain the observed data for two reasons. First, a simple dissociation mechanism predicts that the observed rate will asymptotically approach a limit equal to that for Cu dissociation from holo-Atox1 and become independent of [BCA] (see *SI Text*, *Section B2*). The experimental data do not show this limitation; instead, k_{obs} becomes linearly dependent on [BCA] at high chelator concentrations. Second, the observed rate of "free" Cu uptake by BCA is much slower than any of the rates observed for transfer from Atox1.

The most general mechanism for Cu transfer from holo-Atox1 to BCA involves the following three steps: P = Atox1, L = BCA, X = Cu(I).

$$PX + L \underset{k_{-1}}{\overset{k_1}{\rightleftharpoons}} PXL \underset{k_{-2}}{\overset{k_2}{\rightleftharpoons}} P + XL + L \underset{k_{-3}}{\overset{k_3}{\rightleftharpoons}} LXL \qquad [1]$$

Step 1 involves binding of one BCA to Cu–Atox1 to form the ternary Atox1–Cu–BCA complex (*PXL*), which facilitates dissociation of the protein in step 2 to form the mono-BCA–Cu (*XL*) complex. Step 3 involves the binding of the second BCA molecule to generate the *bis*–BCA–Cu–BCA complex that gives rise to the observed absorbance change. We derived analytical expressions for the equilibrium fraction of Cu–BCA_2 (Y_{LXL}) and the pseudo first order rate constant for transfer (k_{obs}) as function of [BCA or L] and [apo-Atox1 or P], assuming a steady-state assumption for the *PXL* and *XL* intermediates in Eq. 1 (see *SI Text*, *Section A*):

$$Y_{LXL} = \frac{K_1K_2K_3[L]^2}{[P] + K_1[L][P] + K_1K_2[L] + K_1K_2K_3[L]^2} \qquad [2]$$

$$k_{obs} = \frac{k_{-3}k_{-2}(k_{-3} + k_{-1})[P] + k_1k_2k_{-3}[L] + k_1k_{-2}k_{-3}[L][P] + k_1k_2k_3[L]^2}{k_{-2}(k_{-3} + k_{-1})[P] + k_{-3}(k_{-1} + k_2) + k_3(k_{-1} + k_2)[L]} \qquad [3]$$

Both expressions have a dependence on the square of [BCA], accounting for the sigmoidal equilibrium curve and the parabolic dependence of the observed rates of transfer on chelator concentrations. In the case of the kinetic data, Eq. 3 predicts that the y intercept ($[L] \rightarrow 0$) at high P will be k_{-3} and independent of both the nature of the protein and its concentration, which appears to be the case in Figs. 3 and 4. When $[L] \rightarrow \infty$, the expression for k_{obs} becomes:

$$k_{obs} = \frac{k_1k_2[L]}{(k_{-1} + k_2)}. \qquad [4]$$

Eq. **4** predicts a straight line with a slope proportional to $[L]$ and independent of apoprotein concentration, which is also observed experimentally in Fig. 3*B*.

The solid lines in Figs. 3 and 4 represent global fits to combined sets of the equilibrium and kinetic data for three different wild-type apo-Atox1 concentrations and to the two mutant proteins at low protein concentrations. The fitted parameters are reported in Table 1. The correspondence between the observed data and computed lines is remarkably good, suggesting that the ternary mechanism for Cu transfer is valid. The parameters for the last step in Eq. 1 were defined to be the same for all three proteins because they reflect only the rates of binding of the second BCA molecule to the mono-BCA–Cu complex.

There are three main conclusions from this analysis. First, BCA binding to the mono-BCA–Cu complex is roughly 20,000 times faster than to Atox1–Cu (k_3 vs. k_1), and the equilibrium constants for the two BCA-binding steps show roughly the same large differences for all three Atox1 variants (K_3 vs. K_1). Second, the affinity of apo-Atox1 for Cu is much greater than that of BCA (i.e., $1/K_2$ vs. K_1 or K_3), accounting for why an ≈1,000-fold excess of BCA has to be added to extract the metal from the protein. Third, although both mutants transfer Cu more rapidly and have lower affinities (i.e., $1/K_2$) for the metal, the effects of the amino acid replacements are expressed differently in the first two steps. The $Met_{10}Ala$ mutation primarily increases the rate (k_2) and extent (K_2) of Atox1 dissociation from the Atox1–Cu–BCA intermediate and has little effect on the initial binding of BCA. In contrast, the $Lys_{60}Ala$ mutation facilitates the binding of the first BCA molecule (K_1), inhibits BCA dissociation (k_{-1}) and enhances the rate (k_2) and extent (K_2) of Atox1 dissociation from the Atox1–Cu–BCA intermediate.

Discussion

Safe trafficking of Cu in human cells is provided by the metallochaperone Atox1. To date, there is little information on the actual mechanism of Atox1 mediated delivery of Cu to the ATPases, which, in turn, facilitate Cu movement into secretory vesicles for incorporation into target metalloenzymes. Here, we have taken a step toward understanding how Cu–Atox1 can modulate transfer of its metal to potential acceptors, by using the Cu chelator BCA as an initial target. We expected that the reaction of Atox1–Cu with excess BCA would be a relatively simple process limited by the rate of Cu dissociation from the protein (Fig. S2). Instead, the reaction showed a complex parabolic dependence of the observed rate on [BCA].

The observed kinetic and equilibrium patterns require the consecutive reaction of two BCA molecules and transient formation of a ternary Atox1–Cu–BCA complex. The best fits for the observed data were obtained by using the three-step scheme shown in Eq. 1. However, as discussed in *SI Text*, *Section B1*, a two-step mechanism, in which the displacement of Atox1 from the ternary complex is concerted, also provides good fits to the observed data (Fig. S1):

$$PX + L \underset{k_{-1}}{\overset{k_1}{\rightleftharpoons}} PXL + L \underset{k_{-2}}{\overset{k_2}{\rightleftharpoons}} P + LXL. \qquad [5]$$

BIOPHYSICS

The key difference in the 2-step mechanism is that the displacement of Atox1 (P) by the second BCA (L) is a single process involving a quaternary transition state, LPXL, for formation of the final Cu–BCA_2 complex. We chose the three-state model partly because of the lack of precedent for a Cu(I) transition complex with such high order (5 to 6) ligand coordination and, partly, because slightly better fits to the observed data were obtained. However, the two-step process cannot be ruled out.

Regardless of the number of steps in the mechanism, we can conclude that it is much easier for BCA to displace Cu from Met_{10}Ala and Lys_{60}Ala Atox1 than from wild-type Atox1. However, the exact cause of this enhancement in both rate and extent of transfer varies between the two mutants. Previous molecular dynamics (MD) simulations of Met_{10}Ser Atox1 indicated that Met-10 is essential for protein rigidity and for positioning the cysteines in proper orientation for Cu uptake (22). Greater flexibility may help to explain the almost 10-fold greater rate of Atox1 dissociation from the Met_{10}Ala Atox1–Cu–BCA complex (k_2) compared to wild-type protein.

In contrast, the greater ease of Cu displacement from Lys_{60}Ala Atox1 is attributable, in part, to a 4-fold higher affinity of the first BCA for the mutant Atox1–Cu complex. MD simulations of Lys_{60}Ala Atox1 indicate that the protein becomes more rigid, especially the Cu-binding loop, in the absence of Lys-60 (A. Rodriguez-Granillo and P.W.-S., unpublished results). Thus, the Lys_{60}Ala Atox1 mutant may facilitate coordination with the chelator by holding the Cu in place. However, this mutant also dissociates more readily than wild-type Atox1 from the ternary protein–metal–chelator complex (higher K_2 and k_2). In our recent MD study of wild-type Atox1 (30), we found two populations of Cys–Cys distances in the apoprotein, which were designated "open" and "closed." The "open" conformation is expected to release Cu more rapidly, and it is likely that the mutations alter the ratio of these conformers, presumably favoring the "open" form. Testing this interpretation of the higher rates of Cu transfer will require determination of solution structures of the mutants and modeling of their dynamics as well as those of the Atox1–Cu–BCA intermediate.

The initial formation of a ternary complex during the reaction of Atox1–Cu with BCA probably also occurs for Atox1-mediated Cu transfer to the metal-binding domains of ATP7A and ATP7B, although the Cu ligands and coordination geometry likely differ. We speculate that a heterocomplex forms transiently, in which Cu is shared by the Cys in Atox1 and one or two Cys residues in the target domain of the ATP7A/ATP7B proteins. The first metal-binding Cys of the M*XCXX*C motif exhibits greater mobility than the second Cys in all ATPase domains structurally characterized to date (15, 31). Thus, this thiol from a metal-binding domain of WND may form an interaction with the Cu still bound to Atox1, forming a transient three-coordinate intermediate. In support of this idea, NMR studies on Cu(I) glutathione complexes show facile exchange of the metal between thiol ligands through a three coordinate transition intermediate (32). Also, a Cu-dependent transient interaction was observed by NMR between the yeast proteins Atx1 and Ccc2 (33).

The unit cell of the crystal structure of Atox1 contains a Cu bridged homodimer stabilized by intermonomer hydrogen bonds (34). This structure may be a transition state analog of the ternary heteroprotein–metal complex involved in Cu transfer *in vivo* (34), with resemblance to the activated protein–metal–chelator complex. A similar mechanism involving a transient ternary complex has been shown to apply for heme transfer from surface receptors (Shp, Shr) to membrane (apo-HtsA) transporters in *Streptococcus pyogenes*. The heme appears to be transiently shared by axial ligands from both proteins in the activated complex (35, 36).

The dimeric crystal structure of Atox1 raises the possibility that Atox1 may be a dimer in solution, sharing a single Cu atom, and that the first step in the transfer reaction might be displacement of one of the protein molecules by BCA to generate the Atox1–Cu–BCA intermediate. However, as described in the *SI Text*, *Section B3*, this mechanism predicts that the y-axis intercept of plots of k_{obs} vs. [BCA] should depend linearly on free Atox1 concentration (Fig. S3). In contrast, the observed data indicate that the intercept is independent of both [apo-Atox1] and the nature of the protein variant. We also carried out sedimentation velocity experiments to examine the molecular weight of the holoprotein in solution. A single sedimentation coefficient ($s_{20,w}$) of ≈1.15 was observed and is indicative of a monomer, regardless of the absence or presence of Cu. [Runs were performed and analyzed for us by B. Demeler and A. Musatov (University of Texas Health Science Center, San Antonio, TX).] Previous NMR data also shows holo-Atox1 as a monomer in solution (37).

Finally, the slow rate of BCA uptake of Cu(I) from solution containing DTT suggests that Cu chaperones, in addition to facilitating transfer to the correct target, make the metal ions kinetically available to substrate proteins *in vivo*. Millimolar concentrations of strong Cu chelators, such as glutathione, are present in the cytoplasm of eukaryotic cells and would tend to sequester free Cu, inhibiting rapid transport to correct targets (38). To prevent Cu chelation by small molecule thiols, the metal loop in Atox1 appears to have evolved both to sequester Cu(I) and to form transient complexes with acceptor proteins to facilitate rapid and specific metal transfer.

Materials and Methods

Protein Preparation. Met_{10}Ala and Lys_{60}Ala Atox1 variants were created by using the QuikChange site-directed mutagenesis kit in a pET21b vector. Mutations were confirmed by sequencing of the DNA and MALDI-TOF mass spectrometry of purified proteins. Purification of wild-type and Met_{10}Ala Atox1 variants was performed as reported (27). For Lys_{60}Ala Atox1, a pH precipitation step was added to eliminate impurities that could not be separated via gel filtration. Final purity of all proteins was confirmed by SDS/PAGE, which showed single bands. All proteins were purified as apo-proteins; the presence of three reduced Cys in each variant was verified by Ellman's assay. Cu(I) forms were made by using $CuCl_2$ in presence of excess DTT (to keep Cu reduced). The buffer was 20 mM Tris, 150 mM NaCl, and 150–500 μM DTT, pH 7.5.

Equilibrium Experiments. Far-UV CD was measured in a 1-mm cell between 200 and 300 nm; near-UV CD was measured in a 1-cm cell between 250 and 350 nm (J-810 spectropolarimeter, Jasco). Tyrosine fluorescence was measured on a Varian Eclipse (excitation at 280 nm; emission monitored between 290 and 400 nm).

Kinetic Experiments. Cu dissociation from Atox1 variants was studied at 20°C upon mixing holoprotein with increasing concentrations of BCA in a stopped-flow mixer (PiStar, Applied Photophysics). BCA forms a specific 2:1 colored complex with Cu(I) with an $\varepsilon_{562\ nm} = 7.7 \times 10^3\ M^{-1}cm^{-1}$ (25, 39). Change in absorption at 565 nm, indicative of Cu(I)-BCA_2 formation, was followed over time. Final concentrations were 3.3 μM Cu–Atox1 and 0.3 μM apo-Atox1 (to ensure all Cu is in complex with protein at the start); the BCA concentration ranged from 0.3 to 19.8 mM. Additional kinetic experiments were performed with wild-type Atox1 in which the Cu concentration was the same (3.3 μM) but protein concentration was increased to 9 and 15 μM.

SI. *SI Text*, *Section A* contains derivation of analytical expressions for the three-step mechanism, and *SI Text*, *Section B* contains comparison of analytical expressions for three distinct two-step mechanisms. The *SI* also includes Figs. S1–S3 and Tables S1–S3.

ACKNOWLEDGMENTS. We thank Dr. Boris Demeler and Dr. Andrej Musatov (Center for Analytical Ultracentrifugation of Macromolecular Assemblies, University of Texas Health Science Center, San Antonio, TX) for performing analytical ultracentrifugation experiments on apo and various holoforms of Atox1 and Agustina Rodriguez Granillo for MD simulations on Lys_{60}Ala Atox1. P.W.-S. is supported by Robert A. Welch Foundation Grant C-1588. J.S.O. is supported by National Institutes of Health Grants R01 GM035649 and R01 HL047020 and Robert A. Welch Foundation Grant C-0612.

1. O'Halloran TV, Culotta VC (2000) Metallochaperones, an intracellular shuttle service for metal ions. *J Biol Chem* 275:25057–25060.
2. Kulkarni PP, She YM, Smith SD, Roberts EA, Sarkar B (2006) Proteomics of metal transport and metal-associated diseases. *Chemistry* 12:2410–2422.
3. Lamb AL, *et al.* (1999) Crystal structure of the copper chaperone for superoxide dismutase. *Nat Struct Biol* 6:724–729.
4. Lamb AL, Torres AS, O'Halloran TV, Rosenzweig AC (2001) Heterodimeric structure of superoxide dismutase in complex with its metallochaperone. *Nat Struct Biol* 8:751–755.
5. Harrison MD, Jones CE, Solioz M, Dameron CT (2000) Intracellular copper routing: The role of copper chaperones. *Trends Biochem Sci* 25:29–32.
6. Harris ED (2003) Basic and clinical aspects of copper. *Crit Rev Clin Lab Sci* 40:547–586.
7. Hamza I, Schaefer M, Klomp LW, Gitlin JD (1999) Interaction of the copper chaperone HAH1 with the Wilson disease protein is essential for copper homeostasis. *Proc Natl Acad Sci USA* 96:13363–13368.
8. Hung IH, Casareno RL, Labesse G, Mathews FS, Gitlin JD (1998) HAH1 is a copper-binding protein with distinct amino acid residues mediating copper homeostasis and antioxidant defense. *J Biol Chem* 273:1749–1754.
9. Klomp LW, *et al.* (1997) Identification and functional expression of HAH1, a novel human gene involved in copper homeostasis. *J Biol Chem* 272:9221–9226.
10. Hung IH, *et al.* (1997) Biochemical characterization of the Wilson disease protein and functional expression in the yeast Saccharomyces cerevisiae. *J Biol Chem* 272:21461–21466.
11. Hellman NE, *et al.* (2002) Mechanisms of copper incorporation into human ceruloplasmin. *J Biol Chem* 277:46632–46638.
12. Huffman DL, O'Halloran TV (2001) Function, structure, and mechanism of intracellular copper trafficking proteins. *Annu Rev Biochem* 70:677–701.
13. Arnesano F, *et al.* (2002) Metallochaperones and metal-transporting ATPases: A comparative analysis of sequences and structures. *Genome Res* 12:255–271.
14. DeSilva TM, Veglia G, Opella SJ (2005) Solution structures of the reduced and Cu(I) bound forms of the first metal binding sequence of ATP7A associated with Menkes disease. *Proteins* 61:1038–1049.
15. Banci L, Bertini I, Ciofi-Baffoni S, Huffman DL, O'Halloran TV (2001) Solution structure of the yeast copper transporter domain Ccc2a in the apo and Cu(I)-loaded states. *J Biol Chem* 276:8415–8426.
16. Banci L, Bertini I, Del Conte R, Markey J, Ruiz-Duenas FJ (2001) Copper trafficking: The solution structure of Bacillus subtilis CopZ. *Biochemistry* 40:15660–15668.
17. Pufahl RA, *et al.* (1997) Metal ion chaperone function of the soluble Cu(I) receptor Atx1. *Science* 278:853–856.
18. Rosenzweig AC, *et al.* (1999) Crystal structure of the Atx1 metallochaperone protein at 1.02 A resolution. *Structure Fold Des* 7:605–617.
19. Arnesano F, Banci L, Bertini I, Huffman DL, O'Halloran TV (2001) Solution structure of the Cu(I) and apo forms of the yeast metallochaperone, *Atx1*. *Biochemistry* 40:1528–1539.
20. Banci L, Bertini I, Ciofi-Baffoni S, Gonnelli L, Su XC (2003) A core mutation affecting the folding properties of a soluble domain of the ATPase protein CopA from Bacillus subtilis. *J Mol Biol* 331:473–484.
21. Achila D, *et al.* (2006) Structure of human Wilson protein domains 5 and 6 and their interplay with domain 4 and the copper chaperone HAH1 in copper uptake. *Proc Natl Acad Sci USA* 103:5729–5734.
22. Poger D, Fuchs JF, Nedev H, Ferrand M, Crouzy S (2005) Molecular dynamics study of the metallochaperone Hah1 in its apo and Cu(I)-loaded states: Role of the conserved residue M10. *FEBS Lett* 579:5287–5292.
23. Ralle M, Lutsenko S, Blackburn NJ (2003) X-ray absorption spectroscopy of the copper chaperone HAH1 reveals a linear two-coordinate Cu(I) center capable of adduct formation with exogenous thiols and phosphines. *J Biol Chem* 278:23163–23170.
24. Wernimont AK, Yatsunyk LA, Rosenzweig AC (2004) Binding of copper(I) by the Wilson disease protein and its copper chaperone. *J Biol Chem* 279:12269–12276.
25. Yatsunyk LA, Rosenzweig AC (2007) Cu(I) binding and transfer by the N terminus of the Wilson disease protein. *J Biol Chem* 282:8622–8631.
26. Lobley A, Whitmore L, Wallace BA (2002) DICHROWEB: An interactive website for the analysis of protein secondary structure from circular dichroism spectra. *Bioinformatics* 18:211–212.
27. Hussain F, Wittung-Stafshede P (2007) Impact of cofactor on stability of bacterial (CopZ) and human (Atox1) copper chaperones. *Biochim Biophys Acta* 1774:1316–1322.
28. Huffman DL, O'Halloran TV (2000) Energetics of copper trafficking between the Atx1 metallochaperone and the intracellular copper transporter, Ccc2. *J Biol Chem* 275:18611–18614.
29. Walker JM, *et al.* (2004) The N-terminal metal-binding site 2 of the Wilson's disease protein plays a key role in the transfer of copper from Atox1. *J Biol Chem* 279:15376–15384.
30. Rodriguez-Granillo A, Wittung-Stafshede P (2008) Structure and dynamics of Cu(I) binding in copper chaperones Atox1 and CopZ: A computer simulation study. *J Phys Chem B* 112:4583–4593.
31. Banci L, *et al.* (2002) Solution structure of the N-terminal domain of a potential copper-translocating P-type ATPase from Bacillus subtilis in the apo and Cu(I) loaded states. *J Mol Biol* 317:415–429.
32. Cheng C-C, Pai C-H (1998) Specific displacement of glutathione from the Pt(II)-glutathione adduct by Cu(II) in neutral phosphate buffer. *J Inorg Biochem* 71:109–113.
33. Banci L, *et al.* (2006) The Atx1-Ccc2 complex is a metal-mediated protein-protein interaction. *Nat Chem Biol* 2:367–368.
34. Wernimont AK, Huffman DL, Lamb AL, O'Halloran TV, Rosenzweig AC (2000) Structural basis for copper transfer by the metallochaperone for the Menkes/Wilson disease proteins. *Nat Struct Biol* 7:766–771.
35. Nygaard TK, *et al.* (2006) The mechanism of direct heme transfer from the streptococcal cell surface protein Shp to HtsA of the HtsABC transporter. *J Biol Chem* 281:20761–20771.
36. Ran Y, *et al.* (2007) Bis-methionine ligation to heme iron in the streptococcal cell surface protein SHP facilitates rapid hemin transfer to HtsA of the HtsABC transporter. *J Biol Chem* 282:31380–31388.
37. Anastassopoulou I, *et al.* (2004) Solution structure of the apo and copper(I)-loaded human metallochaperone HAH1. *Biochemistry* 43:13046–13053.
38. Meister A (1988) Glutathione metabolism and its selective modification. *J Biol Chem* 263:17205–17208.
39. Brenner AJ, Harris ED (1995) A quantitative test for copper using bicinchoninic acid. *Anal Biochem* 226:80–84.